


## Air sparging as a strategy for optimizing reverse osmosis membrane

Faaz Hussain Saleh<sup>1\*</sup>, Ahmed Faiq Al-Alawy<sup>1</sup> 

<sup>1</sup> Department of Chemical Engineering, College of Engineering, University of Baghdad, Baghdad, Iraq

\* Corresponding author's e-mail: [faaz.salh1607m@coeng.uobaghdad.edu.iq](mailto:faaz.salh1607m@coeng.uobaghdad.edu.iq)

### ABSTRACT

This study aims to enhance the performance of reverse osmosis (RO), a significant membrane technology for water desalination, by improving its permeation flux and rejection of NaCl, which is considered a powerful tool for fouling control. The air sparging approach has been implemented and examined at different air flow rates to achieve this. RO system with air sparging technique has been studied at various operating conditions such as air flow rate range from 1–3 L/min, feed concentration (2000 and 3000 ppm), water flow rate (1 and 1.3 L/min), temperature (20 and 32 °C), and applied pressure (4 and 5 bar). The result confirmed a significant improvement in permeate flux and rejection when the air is injected into the RO system. It revealed that increasing the air flow rate increased the flux, reaching a maximum value at an air flow rate of 1.8 L/min, after that, it started to decline. Additionally, increasing the water flow rate, pressure, and temperature increased the permeate flux. On the other hand, increased feed concentrations negatively impacted the permeate flux. The maximum flux and rejection obtained was 10.76 L/m<sup>2</sup>·hr and 96.17% at 5 bar, 3000 ppm, 1 L/min water flow rate, and T = 32 ± 1 °C. Moreover, the value of the injection factor is equal to 0.64, indicating that the flow pattern was the slug flow, which represented a highly effective flow regime.

**Keywords:** reverse osmosis, air sparging, slug flow, concentration polarization.

### INTRODUCTION

Freshwater depletion is a critical issue worldwide due to the growth of population and economy (Mohammed et al., 2024), which resulted in the exploitation and contamination of natural water resources by industry, agriculture, and urbanization (Biesheuvel et al., 2022; Qasim et al., 2019; Yao et al., 2021). Most current water treatment plants use conventional treatment methods like coagulation-flocculation (Salih et al., 2021), sedimentation, sand filtration, disinfection, and ozonation (Curto et al., 2021; Dimitriou et al., 2017). Membrane technology serves as a productive strategy for groundwater, saline water, and wastewater purification and treatment (Sani et al., 2021; Saleem and Zaidi, 2020). Membrane techniques such as reverse osmosis (RO) are excessively applied for desalination and water treatment, which expeditiously substitutes conventional desalination procedures (Hassan et al., 2024; Joo and Tansel, 2015; Liu et al., 2020).

Reverse osmosis is a pressure-driven operation that uses a semi-permeable membrane for treatment, producing high-quality water (Aliyu et al., 2018). The efficiency of the process depends on operating parameters and membrane and feed water properties (Qadri and Alam, 2024). The membrane modules are divided into four kinds: plate-and-frame, tubular, spiral wound, and hollow fiber. The spiral wound module is the predominant module for nanofiltration or reverse osmosis membrane industriousness because it offers a suitable balance amongst operation, fouling management, permeation rate, and packing density (Haidari et al., 2018; Vinardell et al., 2022).

In the RO process, water (solvent) diffuses throughout the membrane, and the membrane partially or entirely retains the particulate materials (solutes). During the separation process, a boundary layer of concentrated particulate material forms, resulting in the accumulation of particles on the membrane surface. This phenomenon is called concentration polarization. As a

result, fouling is established on the membrane material, and adsorption inside the pores leads to pore blocking (Alsahly et al., 2013; Sivaprakash and DasGupta, 2015; Younos and Tulou, 2009). Concentration polarization and membrane fouling are regarded as the primary restrictions for the membrane-based separation processes. These factors decrease the permeate flux and change the characteristics of the membrane rejection (Fouladitajar et al., 2014).

Numerous equations have been molded to express the mass transfer rate of water and solute through an RO membrane. Eventually, the flux is represented as the product of a mass transfer coefficient and a driving force. The difference between applied and osmotic pressure differentials serves as the driving force for water flow through RO membranes. The equation of water flux ( $J_w$ ) is described as follow (Salih et al., 2023).

$$J_w = K_w(\Delta p - \Delta \pi) \quad (1)$$

where:  $K_w$  is the water permeability constant,  $\Delta p$  is the operating pressure differences, and  $\Delta \pi$  is the osmotic pressure gradient (Critenden, 2012; Salih et al., 2024; Timmer et al., 1993).

The driving force for solute flux is the concentration gradient, and the flux of solutes through RO membranes is described as (Chougradi et al., 2021):

$$J_s = K_s(C_f - C_p) \quad (2)$$

where:  $J_s$  is the solute flux,  $K_s$  is the solute permeability constant,  $C_f$  is feed concentration, and  $C_p$  is permeating concentration.

Fouling control procedures are required to overcome concentration polarization and fouling to minimize the foulants reaching the membrane surface, hold an elevated permeate flux, and recover the natural membrane rejection characteristics. This purpose was achieved by optimization of hydrodynamic situations at the membrane surface by enabling mixing and turbulence flow in the fluid utilizing tube inserts or some structure of vortex mixing approach such as standing vortex waves (Asefi et al., 2019; Choi et al., 2021; Goh et al., 2019).

Gas sparging has been recommended, which may assist in the management of the concentration polarization phenomenon in traditional membrane processes, such as microfiltration (MF), ultrafiltration (UF), nanofiltration (NF), and reverse

osmosis (RO) (Asefi et al., 2019; Vu et al., 2021). The air sparging strategy could be briefly explained by gas bubbles injection into the feed stream during filtration. Then, a gas/liquid two-phase flow is conveyed at the membrane surface. Air sparging is exhibited to be effective with hollow fiber, tubular, or flat sheet membranes (Choi et al., 2021). The technique provides sufficient turbulence and membrane conditioning, which scrubs the particles and other deposited materials far from the surface of the membrane (Park et al., 2010). When liquid and gas flow concurrently in a tube, numerous flow patterns are generated relying on the ratio of air injection, pipe diameter, interfacial tension, and inclination. The injection factor  $\varepsilon$  is used to specify the pattern of two-phase flow in the membrane. This factor is stated as (Fouladitajar et al., 2014):

$$\varepsilon = \frac{U_{GS}}{U_{GS} + U_{LS}} \quad (3)$$

where:  $U_{GS}$  and  $U_{LS}$  are superficial air and liquid velocities, respectively. Bubble flow predominates when the value of  $\varepsilon$  is less than 0.25. As  $\varepsilon$  values extend between 0.25 and 0.9, the system seems to be slug flow, and at higher values, the flow pattern would alter to churn, and finally annular flow.

This study aims to explore the enhancement of reverse osmosis membrane performance through the application of the air sparging technique in the desalination process. The influence of NaCl concentrations, pressure, water flow rate, and temperature on the permeate flux and rejection with and without air sparging has been studied. Additionally, the performance of the RO system was evaluated under two modes of operation: constant feed concentration and variable feed concentration.

## EXPERIMENTAL WORK

### Materials and methods

A spiral wound reverse osmosis membrane module (DuPont Film Tech™: TW30-1812-50HR, USA) has been used to operate in the RO system (with and without air sparging) with an effective area of 0.396 m<sup>2</sup>. NaCl (99.9%, Central Drug House (P) Ltd., India) has been used to prepare the simulated solution.

The experiments were carried out with pilot-scale membrane filtration equipment. A schematic diagram of the apparatus is illustrated in Figure 1. The unit consists of a feed solution prepared in a feed tank with 10 liter capacity by dissolving an amount of NaCl in deionized water. The feed was pumped from a tank to the spiral-wound module by a diaphragm pump (AQUA LOTUS: AQ-400GPD). Three pressure gauges were used to control the air, water, and mixed pressure point. An air flow meter and a water flow meter were used to measure the flow rate of the air and the feed solution, respectively. Isolation valves for air entry and exit with a one-way valve to ensure that the water does not return to the air. The system was operated in two modes: constant feed concentration, the permeate and concentrate stream was recirculated to the feed tank, and variable feed concentration, concentrate is recycled to the feed tank, while permeate is collected individually.

Air and liquid were introduced into the membrane in co-current flow. The flux was obtained as follows (Salih and Al-Alawy, 2022b):

$$Jw = \frac{\Delta V}{A_m \Delta t} \quad (4)$$

where:  $\Delta V$  the volume of water flow from feed to permeate side,  $A_m$  the membrane active area, and  $\Delta t$  the experiment time. The range of the operational conditions was 2000–3000 ppm feed concentrations, 4–5 bar pressure, water flow rate of 0.5–1.3 L/min, air flow rate 1–2.5 L/min,  $20 \pm 1$  and temperature of  $32 \pm 1$  °C. A digital conductivity meter (CRISON: Basic 30, Spain) was used to measure the conductivity of the permeate.

The rejection is calculated from the following equation from the concentrations in feed ( $C_F$ ) and in permeate ( $C_P$ ) (Al-Alawy, 2011; Salih and Al-Alawy, 2022a):

$$Rej = 1 - \frac{C_P}{C_F} \quad (5)$$

## RESULTS AND DISCUSSION

Two preliminary experiments were carried out to examine the influence of using the air sparging technique. One of them was conducted without air injection at an operating condition of 3 bar, 1.05 L/min water flow rate, and 3000 ppm initial concentration. The other one was conducted with an injection of air at an operating condition of 4 bar, 1 L/min water flow rate, 1.8 L/min air flow rate, and 3000 ppm initial concentration. Figure 2 shows the influence of air sparging on the permeate flux. The initial value was 6.06 L/m<sup>2</sup>·hr and reached a maximum value of 6.51 L/m<sup>2</sup>·hr, while without air sparging, a considerable reduction from 5.3 L/m<sup>2</sup>·hr to 3.64 L/m<sup>2</sup>·hr in permeate flux was noticed. These results emphasize that air sparging led to a higher permeate flux in the membrane performance. The injection of air boosts the turbulence movement, which augments the flux because of the back-transport of deposited materials. Therefore, a reduction in concentration polarization is established. Additionally, the aeration of gas bubbles aids in considerable flux modification without impacting the membrane material these results agreed with those obtained by Park et al. (2010), and Sivaprakash and Das-Gupta (2015). These turbulent movements are, to

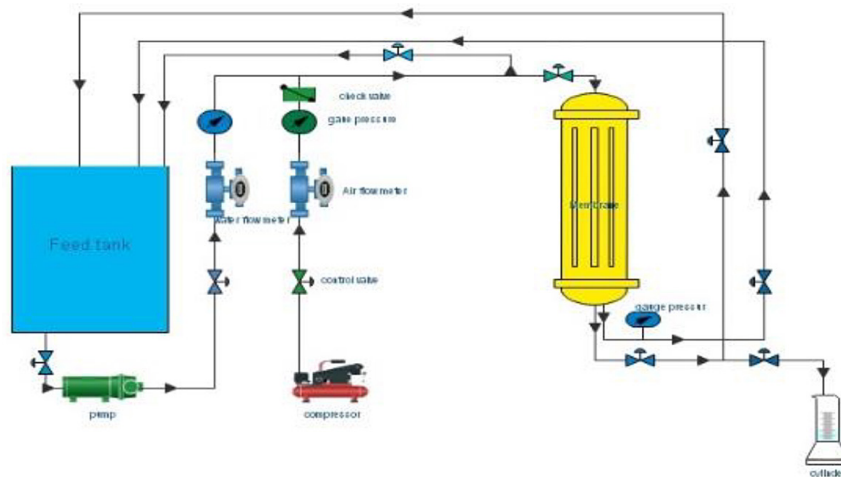
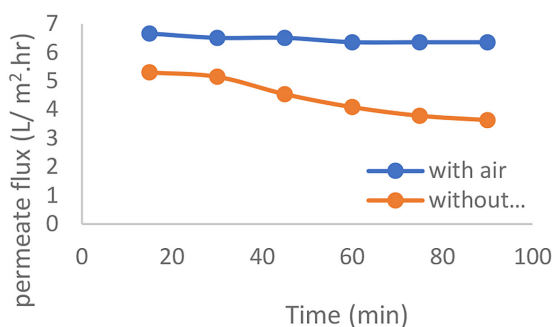


Figure 1. Laboratory scale reverse osmosis with air sparging process



**Figure 2.** Effect of time on permeate flux with and without air sparging at [C = 3000 ppm,  $Q_{H_2O} = 1$  L/min, and  $Q_{air} = 1.8$  L/min]

a certain level, capable of dislocating and removing salt, which possibly would accumulate and partly clog the pores of the channels which was consistent with reported by Psoch and Schiewer (2005). Moreover, an immediate reduction in osmotic pressure occurs after the bubble passes a point on the membrane surface. This reduction is due to a gradual drop in the average concentration when the bubble enters the channel, causing an increase in permeate flux because the bubble sweeps the concentrated liquid from the membrane surface.

The value of the injection factor  $\varepsilon$  calculated from Equation 3 was equal to 0.64, which indicated that the flow pattern represented was the slug flow. For air-sparging, slug flow is a highly effective flow regime for increasing the wall shear stress according to its role in enhancing the cross-flow hydrodynamics around the surface of the membrane that enables maintaining long-lasting permeate fluxes over long periods which was consistent with reported by Psoch and Schiewer (2005). This suggests that slug flow eliminates most solute accumulation near and on the membrane was calculated as mentioned by Vinardell et al. (2022).

The results of rejection are presented in Figure 3, which demonstrates that using air sparging would improve the rejection percentage from 88.1% to 93.7%. Furthermore, it clarifies that NaCl rejection decreases over time when air is not utilized. Conversely, it shows an increase with time when air is used. These observations suggest that gas-liquid two-phase flow could improve the recovery of valuable products or enhance the permeate quality as high rejection is acquired which was consistent with reported by Cui et al. (2003). Figure 4 illustrates the effect of water flow rate on permeate flux at 1 and 1.3 L/min at

various air flow rates (1–3 L/min). The findings showed that at both rates, the permeate flux increased until reaching a certain point representing the maximum flux while the airflow rate ranged from 1–3 L/min. The maximum flux obtained was 6.36 L/m<sup>2</sup>·hr at 1.8 air flow rate and 1 and 1.3 L/min liquid flow rate. After that, the flux began to decrease because, for specific conditions above a critical value, any further increase in air flow rate will not result in any additional enhancement in permeate flux, as mentioned by these results agreed with those obtained by Cui et al. (2003), and Ducom et al. (2002). On the other hand, the rejection increased as the air flow rate increased to 1.8 L/min after that decline. Furthermore, at 1.8 L/min of air flow rate, a slight increase in rejection from 92.76% to 93.03% is noticed when the water flow rate increases from 1 to 1.3 L/min, as depicted in Figure 5.

The enhancement in permeate flux, as the feed flow rate (cross-flow velocity) increased, could be attributed to the fact that the turbulence generated

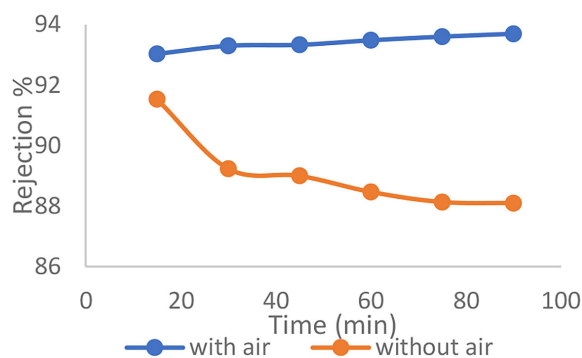


**Figure 3.** Effect of time on rejection with and without air sparging at [C = 3000 ppm,  $Q_{H_2O} = 1$  L/min, and  $Q_{air} = 1.8$  L/min]

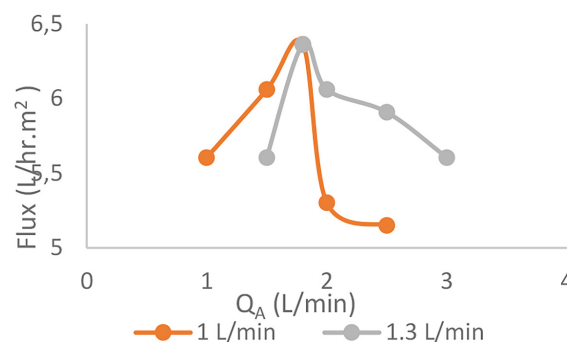


**Figure 4.** Effect of air flow rate on permeate flux at different water flow rates at [P = 4 bar, C = 3000 ppm, and T = 32 ± 1 °C]



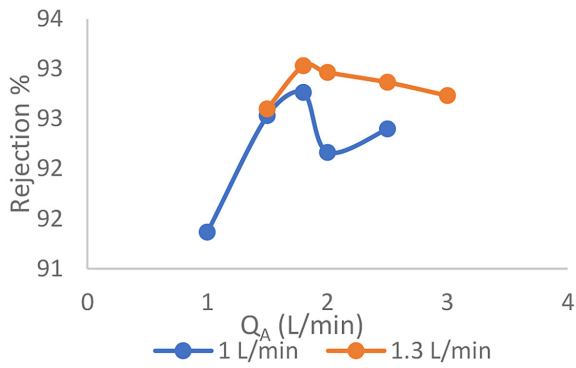


**Figure 5.** Effect of air flow rate on rejection at different water flow rates at [P = 4 bar, C = 3000 ppm, and T = 32 ± 1 °C]

by the fluid pumping has a notable development on permeate flux, as reported by Cheryan (1998). Additionally, when the agitation and mixing of the fluid take place around the membrane surface, the accumulated solute is swept away, a decline in the hydraulic resistance of the cake layer occurs, then decreasing the boundary layer thickness. In any case, this is one of the simplest methods of controlling the effect of concentration polarization. Also Chaudhari observed the same behavior was obtained by Boricha and Murthy (2009). The increase in mass transfer coefficient causes a reduction in concentration polarization and, therefore, a decline in the concentration of NaCl in permeate (C<sub>p</sub>) and this behavior is in agreement with Al-Alawy and Salih (2017), and Boricha and Murthy (2009).

Figure 6 shows the effect of operating pressure on permeate flux. According to water flux (J<sub>w</sub>) equation, the water flux is directly proportionate to the pressure drop over the membrane as reported by Jamal et al. (2004). This behavior is demonstrated by increasing the pressure from 4 to 5 bar, which resulted in increasing the permeate

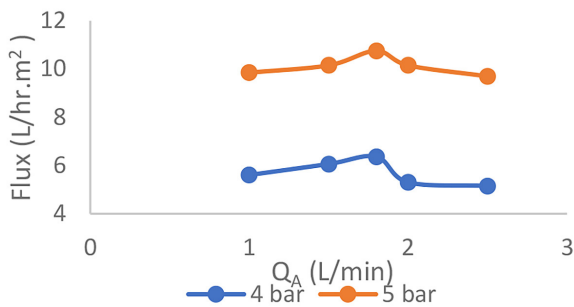


**Figure 6.** Effect of air flow rates on permeate flux at different pressure at [C = 3000 ppm, Q<sub>H<sub>2</sub>O</sub> = 1 L/min, and T = 32 ± 1 °C]

flux from 6.36 to 10.75 L/m<sup>2</sup>·hr at air flow rate of 1.8 L/min. This action is associated with the improvement in the convective flow towards the membrane surface when the pressure increases, thus driving the development of the back diffusion which was consistent with reported by Park and Barnett (2001), and Sivaprakash and Das-Gupta (2015). The difference between applied and osmotic pressure differentials serves as the driving force for water flow.

Figure 7 demonstrates that higher rejection was achieved at a flow rate of 1.8 L/min, increasing from 92.77% to 96.17% as the pressure rose from 4 to 5 bar. This observance is due to the change in the membrane surface, which is associated with a decrease in the average pore size and an improvement in the preferred sorption of pure water at elevated pressures. Therefore, at high pressure, the permeability of solvent rises compared to solute permeability, resulting in augmented rejection which was consistent with reported by Ozaki et al. (2002). At low pressure, the diffusive transport of solute through the membrane surpasses convective transport. When the enforced pressure increases, the reduction in the permeate concentration becomes probable due to convective transport, which poses a significant role at elevated pressure. This outcome was in good agreement with Al-Alawy and Salih (2017).

Figure 8 illustrates the effect of NaCl concentration in the feed on the permeate flux at various rates of air sparging. It can be seen that permeate flux decreases from 9.69 to 6.36 L/m<sup>2</sup>·hr with increasing the concentration of feed from 2000 to 3000 ppm at an air flow rate of 1.8 L/min. Additionally, it can be noticed that in both cases, the maximum flux is obtained when the air flow rate reaches 1.8 L/min. This reduction is similar to that observed by Ujang and Anderson (1998). The

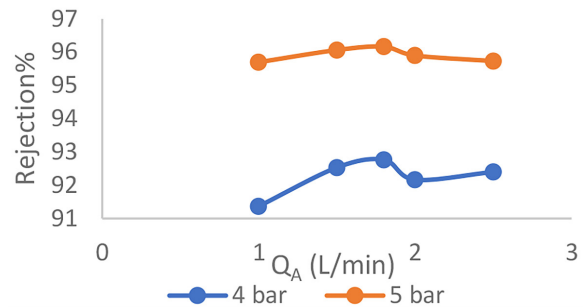


**Figure 7.** Effect of air flow rates on Rejection at different pressure at [C = 3000 ppm, Q<sub>H<sub>2</sub>O</sub> = 1 L/min, and T = 32 ± 1 °C]

concentration polarization development is more prominent with high feed concentration due to the convective transport of both solute and solvent. Moreover, the intermolecular repulsion is superior; that is, the solute permeability rises with an increase in feed concentration, which aligns with the diffusion model given in Equation 2 which was consistent with reported by Ozaki et al. (2002). Consequently, higher NaCl concentration in the feed solution increases the NaCl flux as reported by Jamal et al. (2004). Furthermore, the rising driving potential of the NaCl concentration around the membrane showed the elevation in the osmotic pressure and decrease of water flux according to Equation 1 as reported by Liu et al. (2020). This produces higher rejection which increase from 86% to 92.77% as depicted in Figure 9. Figure 10 indicates the influence of the solution temperature on the reverse osmosis membranes permeate flux. The findings reveal that by increasing the solution temperature from 20 to 32 °C at different air flow rates, the permeate flux rises from 3.48 to 6.36 L/m<sup>2</sup>·hr. Since the solution’s viscosity is reduced at high temperatures, the solution becomes more

accessible to transmit through the membrane, and a higher diffusion rate of water is received. Similar behavior is observed by Wang et al. (2007), and Wei et al. (2013). Conversely, NaCl rejection results will show a decrease from 96.2% to 92.77% as feed temperature increases, as represented in Figure 11. Because more ions will be adsorbed on the membrane surface due to a higher diffusion rate for salt through the membrane and the increase of membrane pore size which was consistent with reported by Al-Mutaz and Al-Ghunaimi (2001).

### Reverse osmosis unit with concentrate recirculation

An experiment of concentrate recirculation was conducted at 2000 ppm initial concentration, 4 bar, 1.8 L/min air flow rate, 1 L/min water flow rate, and 3 hr. to examine the behavior of the RO system in variable feed concentration mode. Figure. 12 presents the flux and permeate concentration as a function of time. It demonstrates that the flux decreases with time, while permeate concentration increases with time. This finding shows an

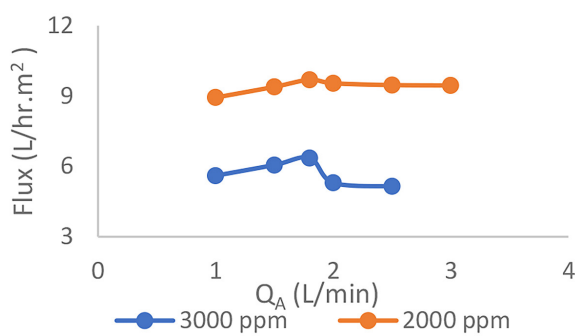


**Figure 8.** Effect of air flow rates on permeate flux at different NaCl concentration at [ P = 4 bar, Q<sub>H<sub>2</sub>O</sub> = 1 L/min, and T = 32 ± 1 °C]

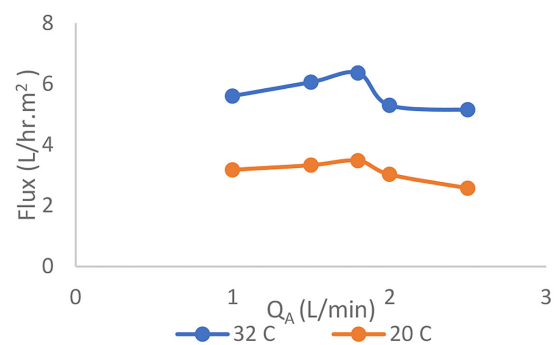


**Figure 10.** Effect of air flow rates on permeate flux at different temperatures [P = 4 bar, Q<sub>H<sub>2</sub>O</sub> = 1 L/min, and C = 3000 ppm]

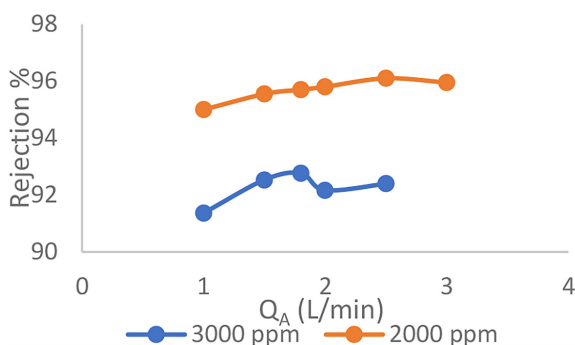


**Figure 9.** Effect of air flow rates on rejection at different NaCl concentration at [P = 4 bar, Q<sub>H<sub>2</sub>O</sub> = 1 L/min, and T = 32 ± 1 °C]

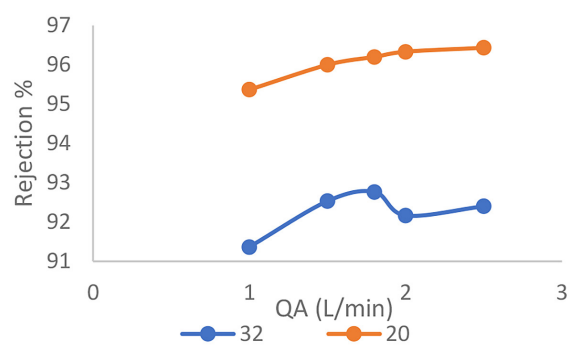


**Figure 11.** Effect of air flow rates on rejection at different temperatures [P = 4 bar, Q<sub>H<sub>2</sub>O</sub> = 1 L/min, and C = 3000 ppm]

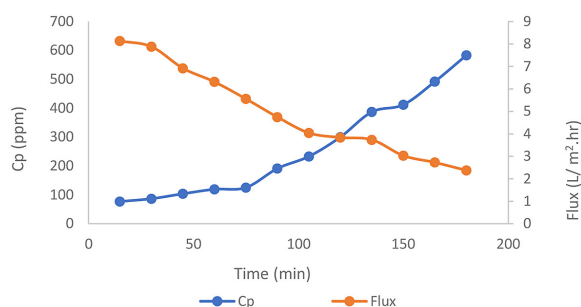


**Figure 12.** Permeate concentration and permeate flux vs time at 2000 ppm initial concentration, 4 bar, 1.8 L/min air flow rate, 1 L/min water flow rate, and 3 hr

opposite effect when compared with the results of the constant feed concentration mode (Figure 2). The permeate concentration raised gradually with the increase in operative time. This behavior is due to the recirculation mode, which resulted in the rise in the feed concentration with time and led to the development of concentration polarization phenomena that caused an increase in the NaCl passage, similar behavior is observed by Wei et al. (2013), and Al-Alawy and Salih (2016). The permeate concentration increased from 77 ppm to 583 ppm over 3 hr.

On the other hand, it appears that the flux diminishes with an increase in operational time. The continuous reduction in the flux was predominantly due to the gradual increase in the solution's viscosity and salt deposition onto the surface of the membrane with a rise in the feed concentration and osmotic pressure, which also develops membrane fouling and intense concentration polarization. Moreover, the increase in osmotic pressure led to a decline in the driving force through the membrane. This behavior is also agreed with. The increase in time to 180 min resulted in a flux reduction to 2.37 L/m<sup>2</sup>·hr.

## CONCLUSION

The air sparging technique proved to be an effective approach, enhancing the performance of the reverse osmosis system compared to operations without air sparging. The results revealed that using air sparging would improve the rejection from 88.1% to 93.7%, and a significant improvement in permeate flux from 3.64 to 6.51 L/hr. m<sup>2</sup> was also observed. Additionally, increasing the water flow rate, pressure, and temperature led to an elevate in the permeate flux. In contrast,

higher feed concentrations negatively impacted the permeate flux. The permeate concentration gradually rises with operating time, while the flux decreases as the operation progresses. The maximum flux has been achieved at an operating condition of 5 bar, 3000 ppm, 1 L/min water flow rate, and T = 32 °C, which was equal to 10.76 L/m<sup>2</sup>·hr. It is noteworthy that in all experiments associated with studying the impact of operational conditions, the maximum flux obtained was always at 1.8 L/min air flow rate, after that, it declined. The results of the constant concentration mode show an opposite effect when compared with the results of the variable concentration mode. gradually with the increase in operative time, while, the flux diminishes with an increase in operational time.

## Acknowledgements

The researcher would like to acknowledge the University of Baghdad, College of Engineering, Chemical Engineering Department for their support in conducting this study

## REFERENCES

1. Al-Alawy, A. F. (2011). Forward and reverse osmosis process for recovery and re-use of water from polluted water by phenol. *Journal of Engineering*, 17(4), 912–928. <https://doi.org/10.31026/j.eng.2011.04.20>
2. Al-Alawy, A. F., & Salih, M. H. (2016). Experimental study and mathematical modelling of zinc removal by reverse osmosis membranes. *Iraqi Journal of Chemical and Petroleum Engineering*, 17(3), 57–73.
3. Al-Alawy, A. F., & Salih, M. H. (2017). Comparative study between nanofiltration and reverse osmosis membranes for the removal of heavy metals from electroplating wastewater. *Journal of Engineering*, 23.
4. Al-Mutaz, I. S., & Al-Ghunaimi, M. A. (2001). Performance of reverse osmosis units at high temperatures. *The Ida World Congress on Desalination and Water Reuse*, 26–31.
5. Aliyu, U. M., Rathilal, S., & Isa, Y. M. (2018). Membrane desalination technologies in water treatment: A review. In *Water Practice and Technology* 13(4), 738–752. IWA Publishing. <https://doi.org/10.2166/wpt.2018.084>
6. Alsally, Q. F., Albyati, T. M., & Zablouk, M. A. (2013). A study of the effect of operating conditions on reverse osmosis membrane performance with and without air sparging technique. *Chemical Engineering Communications*, 200(1), 1–19. <https://doi.org/10.1080/00985965.2013.788888>

- doi.org/10.1080/00986445.2012.685529
7. Asefi, H., Alighardashi, A., Fazeli, M., & Fouladitajar, A. (2019). CFD modeling and simulation of concentration polarization reduction by gas sparging cross-flow nanofiltration. *Journal of Environmental Chemical Engineering*, 7(5). <https://doi.org/10.1016/j.jece.2019.103275>
  8. Biesheuvel, P. M., Dykstra, J. E., Porada, S., & Elimelech, M. (2022). New parametrization method for salt permeability of reverse osmosis desalination membranes. *Journal of Membrane Science Letters*, 2(1), 100010. <https://doi.org/10.1016/j.memlet.2021.100010>
  9. Boricha, A. G., & Murthy, Z. V. P. (2009). Preparation, characterization and performance of nanofiltration membranes for the treatment of electroplating industry effluent. *Separation and Purification Technology*, 65(3), 282–289.
  10. Chaudhary, A. J., Ganguli, B., & Grimes, S. M. (2006). The regeneration and recycle of chromium etching solutions using concentrator cell membrane technology. *Chemosphere*, 62(5), 841–846.
  11. Cheryan, M. (1998). *Ultrafiltration and microfiltration handbook*. CRC press.
  12. Choi, J., Lee, H., & Son, Y. (2021). Effects of gas sparging and mechanical mixing on sonochemical oxidation activity. *Ultrasonics Sonochemistry*, 70(September 2020), 105334. <https://doi.org/10.1016/j.ulsonch.2020.105334>
  13. Chougradi, A., Zaviska, F., Abed, A., Harmand, J., Jellal, J.-E., & Heran, M. (2021). Batch reverse osmosis desalination modeling under a time-dependent pressure profile. *Membranes*, 11(3), 173.
  14. Crittenden, J. C. (2012). *Water treatment principles and design*. John Wiley.
  15. Cui, Z. F., Chang, S., & Fane, A. G. (2003). The use of gas bubbling to enhance membrane processes. In *Journal of Membrane Science* 221(1–2), 1–35. Elsevier. [https://doi.org/10.1016/S0376-7388\(03\)00246-1](https://doi.org/10.1016/S0376-7388(03)00246-1)
  16. Curto, D., Franzitta, V., & Guercio, A. (2021). A review of the water desalination technologies. In *Applied Sciences (Switzerland)* 11(2), 1–36. MDPI AG. <https://doi.org/10.3390/app11020670>
  17. Dimitriou, E., Boutikos, P., Mohamed, E. S., Koziel, S., & Papadakis, G. (2017). Theoretical performance prediction of a reverse osmosis desalination membrane element under variable operating conditions. *Desalination*, 419(November 2016), 70–78. <https://doi.org/10.1016/j.desal.2017.06.001>
  18. Ducom, G., Matamoros, H., & Cabassud, C. (2002). Air sparging for flux enhancement in nanofiltration membranes: Application to O/W stabilised and non-stabilised emulsions. *Journal of Membrane Science*, 204(1–2), 221–236. [https://doi.org/10.1016/S0376-7388\(02\)00044-3](https://doi.org/10.1016/S0376-7388(02)00044-3)
  19. Fouladitajar, A., Zokae Ashtiani, F., Rezaei, H., Haghmoradi, A., & Kargari, A. (2014). Gas sparging to enhance permeate flux and reduce fouling resistances in cross flow microfiltration. *Journal of Industrial and Engineering Chemistry*, 20(2), 624–632. <https://doi.org/10.1016/j.jiec.2013.05.025>
  20. Goh, P. S., Zulhairun, A. K., Ismail, A. F., & Hilal, N. (2019). Contemporary antibiofouling modifications of reverse osmosis desalination membrane: A review. *Desalination*, 468(April). <https://doi.org/10.1016/j.desal.2019.114072>
  21. Golrokh Sani, A., Najafi, H., & Azimi, S. S. (2021). CFD simulation of air-sparged slug flow in the flat-sheet membrane: A concentration polarization study. *Separation and Purification Technology*, 270. <https://doi.org/10.1016/j.seppur.2021.118816>
  22. Haidari, A. H., Heijman, S. G. J., & van der Meer, W. G. J. (2018). Optimal design of spacers in reverse osmosis. In *Separation and Purification Technology* 192, 441–456. Elsevier B.V. <https://doi.org/10.1016/j.seppur.2017.10.042>
  23. Hassan, H. A., Al-Alawy, A. F., & Al-shaeli, M. (2024). Utilizing hybrid RO-OARO systems as new methods for desalination process. *Iraqi Journal of Chemical and Petroleum Engineering*, 25(1), 23–35. <https://doi.org/10.31699/ijcpe.2024.1.3>
  24. Jamal, K., Khan, M. A., & Kamil, M. (2004). Mathematical modeling of reverse osmosis systems. *Desalination*, 160(1), 29–42. [https://doi.org/10.1016/S0011-9164\(04\)90015-X](https://doi.org/10.1016/S0011-9164(04)90015-X)
  25. Joo, S. H., & Tansel, B. (2015). Novel technologies for reverse osmosis concentrate treatment: A review. In *Journal of Environmental Management* 150, 322–335. Academic Press. <https://doi.org/10.1016/j.jenvman.2014.10.027>
  26. Liu, H., Gu, J., Wang, S., Zhang, M., & Liu, Y. (2020). Performance, membrane fouling control and cost analysis of an integrated anaerobic fixed-film MBR and reverse osmosis process for municipal wastewater reclamation to NEWater-like product water. *Journal of Membrane Science*, 593(August 2019), 117442. <https://doi.org/10.1016/j.memsci.2019.117442>
  27. Mohammed, H. K., Al-Alawy, A. F., Abbas, T. R., Al-Mosawi, A. I., & Salih, M. H. (2024). Mathematical modeling of osmotic membrane bioreactor process for oily wastewater treatment. *Water Science and Technology*, 90(7), 2234–2250. <https://doi.org/10.2166/wst.2024.318>
  28. Ozaki, H., Sharmab, K., & Saktaywirf, W. (2002). DESALINATION Performance of an ultra-low-pressure reverse osmosis membrane (ULPROM) for separating heavy metal: effects of interference parameters. *Desalination*, 144, 287–294.



29. Park, E., & Barnett, S. M. (2001). Oil/water separation using nanofiltration membrane technology. *Separation Science and Technology*, 36(7), 1527–1542. <https://doi.org/10.1081/SS-100103886>
30. Park, H. D., Lee, Y. H., Kim, H. B., Moon, J., Ahn, C. H., Kim, K. T., & Kang, M. S. (2010). Reduction of membrane fouling by simultaneous upward and downward air sparging in a pilot-scale submerged membrane bioreactor treating municipal wastewater. *Desalination*, 251(1–3), 75–82. <https://doi.org/10.1016/j.desal.2009.09.140>
31. Psoch, C., & Schiewer, S. (2005). Critical flux aspect of air sparging and backflushing on membrane bioreactors. *Desalination*, 175, 61–71. <https://doi.org/10.1016/j.desal.2005.09.014>
32. Qadri, A., & Alam, M. (2024). Drinking water treatment using advanced oxidation processes. *International Journal of Chemical and Biochemical Sciences*, 25(14), 154–163. <https://www.iscientific.org/wp-content/uploads/2024/03/19-IJCBS-24-25-14-19.pdf>
33. Qasim, M., Badrelzaman, M., Darwish, N. N., Darwish, N. A., & Hilal, N. (2019). Reverse Osmosis Desalination: A State-of-the-Art Review. *Desalination*, 459, 59–104.
34. Saleem, H., & Zaidi, S. J. (2020). Nanoparticles in reverse osmosis membranes for desalination: A state of the art review. *Desalination*, 475(October 2019), 114171. <https://doi.org/10.1016/j.desal.2019.114171>
35. Salih, M. H., & Al-Alawy, A. F. (2022a). A novel forward osmosis for treatment of high-salinity East Baghdad oilfield produced water as a part of a zero liquid discharge system. *Desalination and Water Treatment*, 248, 18–27. <https://doi.org/10.5004/dwt.2022.28070>
36. Salih, M. H., & Al-Alawy, A. F. (2022b). MgCl<sub>2</sub> and MgSO<sub>4</sub> as draw agents in forward osmosis process for East Baghdad oilfield produced water treatment. *Desalination and Water Treatment*, 256, 80–88. <https://doi.org/10.5004/dwt.2022.28408>
37. Salih, M. H., Al-Alawy, A. F., & Ahmed, T. A. (2021). Oil skimming followed by coagulation/flocculation processes for oilfield produced water treatment and zero liquid discharge system application. *AIP Conference Proceedings*, 2372(November). <https://doi.org/10.1063/5.0065365>
38. Salih, M. H., Al-Yaqoobi, A. M., Hassan, H. A., & Al-Alawy, A. F. (2023). Assessment of the Pressure Driven Membrane for the Potential Removal of Aniline from Wastewater. *Journal of Ecological Engineering*, 24(8), 118–127. <https://doi.org/10.12911/22998993/166283>
39. Salih, M. H., Hassan, H. A., Al-Alawy, R. M., Zaboon, S., Al-Alawy, A. F., & Al-Jendeel, H. A. (2024). Green power generation from the Tigris River using pressure retarded osmosis process. *Desalination and Water Treatment*, 320(June), 100887. <https://doi.org/10.1016/j.dwt.2024.100887>
40. Sivaprakash, P., & DasGupta, S. (2015). Effect of air sparging on flux enhancement during tangential flow filtration of degreasing effluent. *Desalination and Water Treatment*, 53(1), 73–83. <https://doi.org/10.1080/19443994.2013.839400>
41. Timmer, J. M. K., Van Der Horst, H. C., & Robbertsen, T. (1993). Transport of lactic acid through reverse osmosis and nanofiltration membranes. In *Journal of Membrane Science* 85.
42. Ujang, Z., & Anderson, G. K. (1998). Performance of low pressure reverse osmosis membrane (LPRO) for separating mono- and divalent ions. *Water Science and Technology*, 38(4–5–5 pt 4), 521–528. [https://doi.org/10.1016/S0273-1223\(98\)00553-8](https://doi.org/10.1016/S0273-1223(98)00553-8)
43. Vinardell, S., Sanchez, L., Astals, S., Mata-Alvarez, J., Dosta, J., Heran, M., & Lesage, G. (2022). Impact of permeate flux and gas sparging rate on membrane performance and process economics of granular anaerobic membrane bioreactors. *Science of the Total Environment*, 825, 153907. <https://doi.org/10.1016/j.scitotenv.2022.153907>
44. Vu, M. T., Nguyen, L. N., Johir, M. A. H., Zhang, X., Long, D. N., & Elimelech, M. (2021). Biogas sparging to control fouling and enhance resource recovery from anaerobically digested sludge concentrate by forward osmosis. *Journal of Membrane Science*, 0–22.
45. Wang, Z., Liu, G., Fan, Z., Yang, X., Wang, J., & Wang, S. (2007). Experimental study on treatment of electroplating wastewater by nanofiltration. *Journal of Membrane Science*, 305(1–2), 185–195.
46. Wei, X., Kong, X., Wang, S., Xiang, H., Wang, J., & Chen, J. (2013). Removal of heavy metals from electroplating wastewater by thin-film composite nanofiltration hollow-fiber membranes. *Industrial & Engineering Chemistry Research*, 52(49), 17583–17590.
47. Yao, Y., Zhang, P., Jiang, C., DuChanois, R. M., Zhang, X., & Elimelech, M. (2021). High performance polyester reverse osmosis desalination membrane with chlorine resistance. *Nature Sustainability*, 4(2), 138–146. <https://doi.org/10.1038/s41893-020-00619-w>
48. Younos, T., & Tulou, K. E. (2009). Overview of Desalination Techniques. *Journal of Contemporary Water Research & Education*, 132(1), 3–10. <https://doi.org/10.1111/j.1936-704x.2005.mp132001002.x>